Powering and Communicating with mm-size Implants

Jan M. Rabaey, Michael Mark, David Chen, Christopher Sutardja,
Chongxuan Tang, Suraj Gowda, Mark Wagner and Dan Werthimer
University of California at Berkeley
Berkeley Wireless Research Center
Berkeley, CA, USA
jan@eecs.berkeley.edu

***Abstract*—This paper deals with system level design considerations for mm-size implantable electronic devices with wireless connectivity. In particular, it focuses on neural sensors as one application requiring such miniature interfaces. Common to all these implants is the need for power supply and a wireless interface. Wireless power transfer via electromagnetic fields is identified as a promising option for powering such devices. Design methodologies, system level trade-offs, as well as limitations of power supply systems based on electromagnetic coupling are discussed in detail. Further, various wireless data communication architectures are evaluated for their feasibility in the application. Reflective impulse radios are proposed as an alternative scheme for enabling highly scalable data transmission at <1pJ/bit. Finally, design considerations for the corresponding reader system are addressed.**

Keywords-component; implantable neural sensors, brain-machine interfaces, wireless power transfer, ultra low power, data communication

I. INTRODUCTION

Recent advances in neuroscience and engineering utilizing miniature, implantable neural sensors have the potential to make substantial difference in the lives of millions who are paralyzed or have suffered a devastating stroke or the loss of a limb. Although Brain-Machine Interfaces (BMI) is a young multidisciplinary field, it has enormous potential as a therapeutic technology that will improve the quality of life for the physically impaired, and has grown tremendously during the last decade.

BMI is about transforming thought into action, or conversely, sensation into perception [1]. For it to make the step from laboratory experiments on animals to true deployment in humans, dramatic improvement is required in the power and data transmission interface. Neural sensing nodes should be of the size of a few mm^3, communicate with the outside world wirelessly, and be completely self-contained from an energy perspective. The small size, combined with safety regulations, puts an upper limit on the power available for establishing wireless connectivity and performing additional tasks such as data acquisition. It is therefore critical to co-design the power delivery and data transmission sub-systems that provide a maximum amount of power per area to the rest of the system. Due to the broad range of application bases that can benefit from such wireless implants, the exact size of the implanted device also varies substantially. In some applications neural probes of 10s of mm^2 large are used [2]; in others, much smaller systems are desirable to enable chronic recordings by minimizing micromotion in vivo [3]. This paper therefore focuses on designing and optimizing power supply and data transmission for implants of scalable size from 10x10 mm^2 down to 1x1 mm^2.

After this brief introduction, section II of this paper looks at different powering options for implants and subsequently focuses on wireless power transfer through electromagnetic fields as currently the most promising option for these applications. A Computer Aided Design (CAD) based design methodology for finding optimal antenna size and frequency of operation pairs is introduced and challenges and limitations, both from a system's, as well as from a circuit's point of view are discussed. Some system level approaches increasing the RF-to-DC conversion efficiency are introduced, increasing the amount of power available to the implant substantially. Section III presents the inherent link asymmetry in wireless data communication then compares radio frequency identification (RFID) and ultra wide-band (UWB), two primary technologies for ultra low power data transmission. Reflective impulse radios (RIR) are subsequently proposed as an alternative architecture for supporting highly scalable data rate at less than 1 pJ/bit energy consumption. Advantages of using RIR for mm-size neural implants are also demonstrated. Section IV of the paper discusses the trade-offs in implementing the external reader system, which carries the dual function of power transmission and data receiving. Section V provides a brief conclusion.

II. POWER DELIVERY

A. Power Sources for Implants

Table I lists possible power sources for implantable devices. Commonly used in implantable applications such as cardiac pacemakers, batteries are the most obvious choice. The challenge however is that they usually require some sort of encapsulation and therefore do not scale well down to the mm-size. Additionally, their power density is rather low and their limited cycle time requires replacement surgeries on a regular basis, which is obviously undesirable. Energy harvesting within the body could potentially eliminate the need for replacing the battery and is thus a very interesting alternative. The challenge however is the current state of the technology where both, its power density and longevity, remain insufficient for miniature implants [5-7]. Finally, electromagnetic power transfer, where an external transmitter generates an electromagnetic field that

978-3-9810801-7-9/DATE11/©2011 EDAA

TABLE I. POWER DENSITIES OF VARIOUS ENERGY SOURCES

Principle and Constraints	Powerdensity
Primary batteries [4]	0.09 μW/mm^2/year
Glucose bio-fuel cell utilizing glucose from blood (5 mM) [5]	2.8 μW/mm^2
Thermoelectric, ΔT=5°C [6]	0.6 μW/mm^2
Piezoelectric microbender, f ≈ 800 Hz, 2.25 m/s^2 [7]	< 0.2 μW/mm^3
Electromagnetic power transfer	10 to 1000 μW/mm^2

is harvested by the implanted device, demonstrates the highest power density. Without any moving parts or the need for chemical processing or temperature gradient, it is also a more robust solution, proven in cochlear implants. The rest of this section will therefore focus on electromagnetic-based powering options.

B. Electromagnetic Power Transfer Through Tissue

Most remotely powered implants are operating at carrier frequencies at or below a few MHz [8]. However, recent research has shown that, for very small receive antenna sizes, the optimum frequency that minimizes the link loss can be significantly higher [9]. Since the interaction between electromagnetic field and biological tissue increases with frequency, a good understanding and accurate modeling of the wireless channel is important to design reliable radio links at high frequencies.

A modeling approach based on dielectric properties of tissue has been introduced and verified by measurements in animals [10]. It has subsequently been used to optimize various aspects of the wireless link including the antenna [11]. Typically, loop antenna structures are preferred when powering implanted devices, thanks to their good magnetic coupling properties and low electric near fields [9, 11]. Furthermore it has been shown that, for a given receive antenna geometry and separation from the power transmit antenna, there exists an optimum transmit antenna size and a corresponding optimum operating frequency that minimizes the coupling losses [11].

Figures 1 and 2 show the maximum achievable coupling

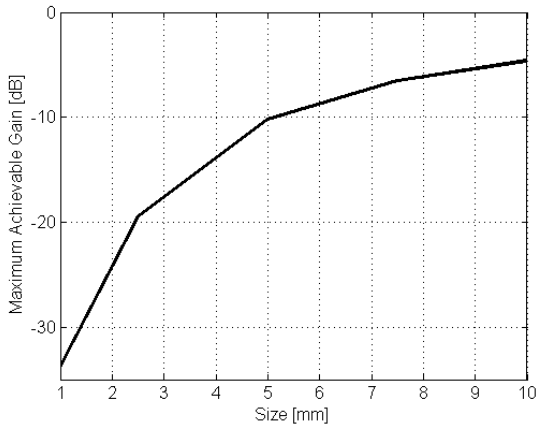

Figure 1. Coupling vs. receive antenna size

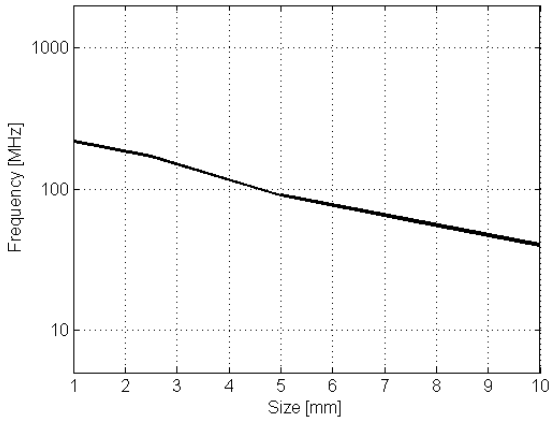

Figure 2. Optimum frequency vs. receive antenna size

and the optimum frequency as a function of the receive antenna's outer dimension, respectively. Additional assumptions are made as follows:

- Receive antenna: a single loop square with trace width 1/10 of its outer dimension;
- Transmit antenna: a single turn hexagonal loop with size optimized for each receive antenna case;
- Layered channel model: 5 mm of air, 2 mm of skin, 2 mm of fat, and 7 mm of bone [10].

While the actual values of the results may vary significantly with the actual implementation of the various antennas (especially for the larger size ones, due to the higher flexibility e.g. in terms of number of turns and trace width), the trends described in the following sections will still hold.

As can be observed from Figure 1, the achievable coupling is a strong function of size and degenerates heavily for antennas smaller than 4x4 mm^2. At the same time, the optimum frequency increases with decreasing size, as shown in Figure 2. When moving to smaller receiver sizes and therefore higher frequencies, the optimum transmit antenna sizes also reduced, although less drastically (from approximately 2.5 cm to 2 cm).

Besides size, the other limitation on the received power comes from the maximum power allowed for transmission for health concerns. Although viewed controversial by some, there exist various regulations that limit the maximum electromagnetic fields to which the human body can be exposed. The regulatory limits for cell phones for example are based on the specific absorption rate (SAR) averaged over a certain mass of tissue. Since the actual values vary from region to region, U.S. regulations were used to compute the lower bound of the maximum transmit power, since they are more stringent than others (the SAR value for partial body exposure is 1.6 W/kg over 1 gram of tissue in the U.S. [12] in contrast to 2 W/kg over 10 gram in Europe [13]).

The built-in SAR function of Ansoft HFSS was used to simulate the local SAR values, and averaging was performed in Matlab. Figure 3 shows the received power for a given receive antenna dimension at the maximum coupling point. It ranges from a few 100 mW for 10x10 mm^2 to as little as 10s of μW for the 1x1 mm^2 nodes. The second curve shows the maximum

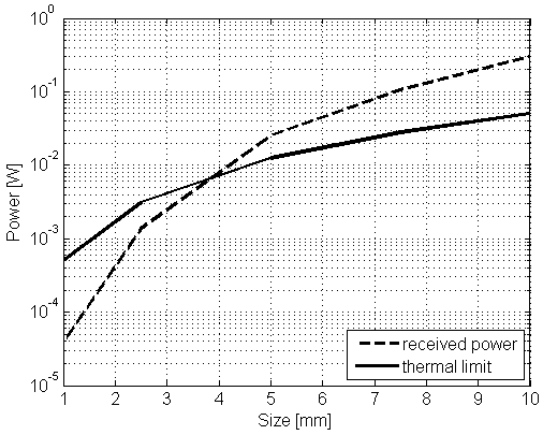

Figure 3. Received power vs. receive antenna size

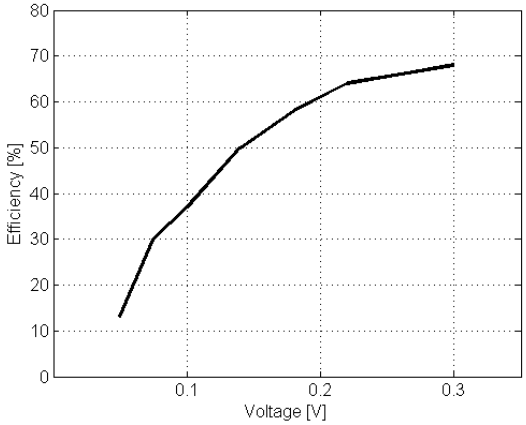

Figure 4. Rectifer efficiency vs. peak input voltage

power consumption for implantable integrated circuits of a given size that produces an amount of tissue heating comparable to the one leading to the SAR limitations. Research has shown that a power density of approximately 500 μW/mm^2 leads to a 1º C increase in temperature in the surrounding tissue [14]. It can therefore be concluded that the maximum power allowed for implanted electronics larger than approximately 4x4 mm^2 is not limited by the power transfer, but rather by the intrinsic heating of the device itself..

In the power-transfer limited regime, additional design choices can be made to trade e.g. coupling efficiency for maximum received power. The fact that coupling efficiency with respect to both, the optimum frequency and the optimum transmit antenna size, exhibits rather broad optima provides possibility for such trade-offs. All following parameters – frequency, transmit antenna geometry and its distance from the human body – can be adjusted to increase the received power at the cost of reduced coupling. At lower frequencies, the SAR caused by a fixed antenna geometry is typically lower and the transmit power can therefore be increased. Similarly, a larger transmit antenna spatially spreads the fields the human body is exposed to, therefore reducing the SAR averaged over a certain mass of tissue. Finally, moving the transmitter further away from the human body reduces the SAR as well [11]. The values plotted in Figures 1 to 3 are therefore by no means hard limits; but serve as indicators for the main trends.

C. Circuit Level Implications

Once the electromagnetic energy is received by the antenna of the implant the alternating signal needs to be converted into a stable DC supply voltage. Depending on the function and the actual circuit implementations, a stable DC supply voltage of at least 0.5 V is needed [15]. The minimum configuration of a power supply block of a remotely-powered implant consists therefore of a rectifier, converting the incoming AC signal into DC, a reference voltage and a voltage regulator, to generate an accurate and stable supply voltage. At different input power levels, several stages of voltage multiplication may be needed in the rectifier to achieve the desired minimum DC output voltage.

To maximize the power available for conversion, it is crucial that the input impedance of the rectifier is matched to the impedance of the antenna. Moreover, the rectifier efficiency is a strong function of the actual input voltage. Figure 4 shows the efficiency of a generic self-synchronous rectifier [16] simulated in 65 nm CMOS over an input peak voltage range from 50 mV to 300 mV. While the shown curve is for one particular implementation, virtually all rectifier architectures exhibit a similar behavior. In fact the chosen self-synchronous architecture is one that has been proven to be particularly efficient at low input voltages [16]. For any system, it is therefore important to maximize the input voltage for a given receive power. For a fixed amount of power, the voltage seen across the antenna can be increased by raising the antenna impedance. To achieve this, the loop antenna, which is usually inductive at the frequency of interest, is resonated out by a low loss capacitor in parallel with the input capacitance of the integrated circuit. The real part of the input impedance is then designed to match the resonant impedance of the antenna under maximum load condition.

Efficiently converting the available power to a DC voltage becomes especially difficult at very small antenna sizes. On one hand the received power is very low already, and on the other hand the maximum achievable impedance of the antenna, and therefore the voltage, is rather low as well. In the case of 1x1 mm antenna, the resonant impedance is only about 50 Ohms. Paired with the simulated receive power of approximately 40 μW, this leads to an input peak voltage of merely 60 mV, which results in only 15% of rectifier-efficiency according to Figure 4. With additional losses from the resonant capacitors and the voltage regulator, the DC output available for the implant may not be much more than 3 μW. Operating at a higher frequency provides only limited benefits, since the maximum allowed transmit power is inversely proportional to the frequency, almost completely offsetting the gain from increased antenna impedance and input voltage.

One approach that shows great potential is to duty cycle the power transmission. The SAR constraints are derived based on a certain increase in temperature in the tissue affected by the electromagnetic fields. If the power transmission is duty cycled, the tissues can cool down and the heat can diffuse

during the off period. Several recommendations, such as the IEEE C95.3, take this into account and specify time averaged values for their maximum E- and H-field recommendations [17]. While the exact timing and power levels of the duty cycling have to be determined based on thermal simulation, a simple first order analysis demonstrates how this approach can be used to increase the DC power available to the implant. If, for example, 25 times the maximum transmit power is transmitted, the input peak voltage increases from 60 mV to 300 mV, increasing the rectifier efficiency with a factor 5. In order to expose the tissue to the same average amount of electromagnetic fields, this large power can only be transmitted for $1/25^{th}$ of the time. During that time an on-chip capacitor can be charged, serving as energy reservoir for the time the power pulse is turned off. This way the DC power available to the implant can be increase drastically. As an additional benefit, since the input voltage is higher, less stages of voltage multiplication in the rectifier are needed, leading to a reduction in circuit complexity and size. The major drawback of this approach is that depending on the actual duty cycle and the power consumption of the device the on-chip storage capacitor can be quite large.

III. DATA TRANSMISSION

Similar to powering, the throughput required for data transmission scales with the sensor size too. Additionally it also depends on the level of in-sensor data compression: raw recording (no compression), spike extraction (about 15x data reduction [18]), and spike detection and sorting (an additional 10x data reduction [19]). Figure 5 shows the required data rate for all three scenarios at sizes from 1×1 mm^2 to 10×10 mm^2. The range extends from 30kbps up to 500Mbps, assuming in the highest data rate case: 4 electrodes per mm^2, 4 recording sites per electrode, and 10-bit ADC at 32 kSps. Coupled with the limited amount of power available, this represents a severe challenge to data transmission.

A. Link Asymmetry

The data transmission challenge presented in neural sensors is in fact common to many emerging wireless sensor network applications. While the data receiver may be allowed with more power and bigger size, the transmitter is less resourceful

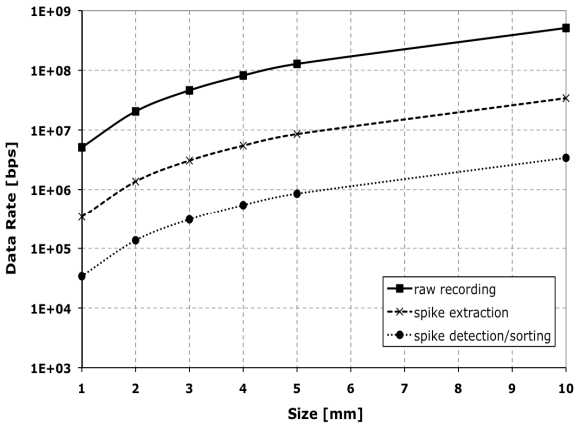

Figure 5. Data rate vs. size for three compression scenarios

(Table II). In other words, there exists a major degree of link asymmetry. Any architectural arrangement that can reduce the power consumption of the transmitter, even at the expense of the receiver, is thus a worthwhile trade-off.

TABLE II. DATA TRANSMITTER AND RECEIVER COMPARISON

	Location	***Power***	***Size***
Transmitter	In vivo	1μW	$1mm^3$
Receiver	Extracutaneous	> 100mW	> $1cm^3$

Both UWB and RFID are technologies designed for ultra low power data transmission. An UWB transmitter is highly efficient on the energy per bit basis, by shifting the burden of clock recovery and pulse detection to its receiver. An RFID tag consumes even less amount of power, although at a much reduced data rate. Table III lists the performance summary of both technologies.

TABLE III. PERFORMANCE OF UWB AND RFID TECHNOLOGIES [20-22]

	Transmitter Power	***Data Rate***
UWB	> 0.6mW	Up to 500Mbps
RFID	< 5μW	Up to several hundred kbps

Unfortunately, the requirements placed upon miniature neural sensors extend beyond what is possible with technologies summarized in Table III. The $1mm^2$ node for example calls for <5μW power consumption, precluding UWB. Its need for up to 5 Mbps also exceeds the capability of conventional RFID. An alternative solution is clearly needed.

B. Reflective Impulse Radios

An alternative communication architecture named "Reflective Impulse Radios (RIR)" is hereby proposed. It combines the backscattering scheme of RFID and pulse-based modulation of UWB, hence maintaining the low power feature of an RFID tag but at an elevated data rate. Figure 6 illustrates the operation of an RIR radio. The dark sinusoid represents the continuous wave from the reader (or interrogator in RFID terminology). Similar to an RFID tag, a switch is connected across the transmitter antenna, where the rectangular waveform represents the switch's control signal. The reflected wave is the gray curve, the amplitude of which varies based on the control signal above.

Due to narrow pulse width of the control signal, the spectral bandwidth of the reflected wave is relatively broad. This is shown in the lower half of Figure 6. The dark impulse at carrier frequency f_C represents the continuous wave sinusoid. The rest of the plot in gray depicts the power spectral density (PSD) of the reflected data signal, where mathematically

$$\ldots = f_2 - f_1 = f_1 - f_C = f_C - f_{-1} = \ldots = \frac{1}{t_2 - t_1} = \frac{1}{t_4 - t_3} = \ldots \qquad (1)$$

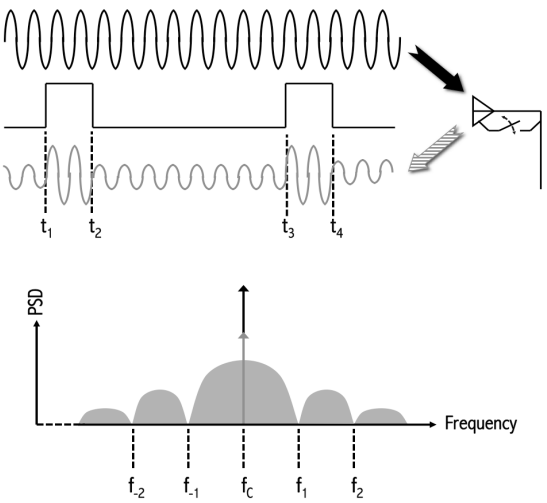

Figure 6. Concept of reflective impulse radios

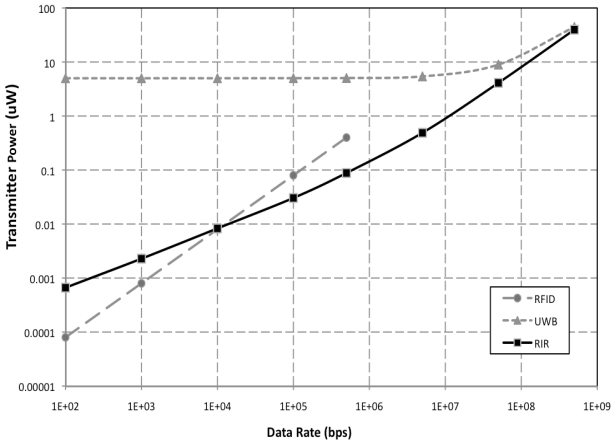

Figure 7. Comparative advantges of reflective impulse radios

RIR is a hybrid of passive transmission and impulse modulation, which not only enables high throughput but also allows the transmitter to turn itself off during most of the most time when it is not transmitting so that its average power consumption is comparable to that of an RFID tag. Additionally, the antenna of an RIR transmitter does not need to be as broadband as that for UWB. By directly modulating the antenna with a switch across it, an RIR transmitter extends the effective bandwidth of the antenna by as much as 30x [23-25]. An otherwise narrow-band antenna intended for RFID applications can, for instance, be readily suitable for RIR.

C. Comparative Advantages

To evaluate the comparative advantages of the new radio architecture, following assumptions are made:

- Both RFID and RIR rectify incident RF carrier to DC power when the antenna switch is turned off;
- Both UWB and RIR have the same spectral profile and transmit an equal amount of energy per bit;
- The RFID tag operates under on-off keying (OOK) modulation with signaling bandwidth ≤ 1MHz;
- Other circuit parameters are based on a commercial 65nm CMOS process.

Under above assumptions, Figure 7 compares the power consumption of an RIR transmitter to UWB and RFID. RFID consumes less power below 10 kbps as the local oscillator on the tag operates at a much lower frequency than in the RIR transmitters. At higher data rates however, far less energy is available for rectification in RFID than in RIR, offsetting the power savings in the oscillator. The power of an UWB transmitter is unconditionally higher than RIR, because of inherent inefficiency in the power amplifier and the RF-to-DC rectifier. RIR transmitters hence have a clear advantage for data rates higher than 10 kbps. Its theoretical power consumption is 1μW at 8Mbps or 125fJ/b, meeting the stringent requirements of mm-size neural implants.

IV. READER DESIGN

The extracutaneous reader serves two purposes in the neural recording system. First, it provides power to illuminate the sensor in vivo. Second it decodes the signals received from the RIR transmitter. Figure 8 shows the block diagram of a potential reader architecture. The circulator prevents, to some degree, the outbound power from interfering with the reflected signal. Remaining part of the self interference is further attenuated by the jammer cancellation branch consisting of the directional coupler, a programmable attenuator, a programmable phase shifter, and a hybrid power combiner (all in gray in Figure 8).

While Figure 8 resembles the block diagram of an RFID reader, key differences exist. All components along the data receiving path, including the antenna and matching network, need to be broadband. Otherwise there can be two adverse consequences: reduction of signal power and increase of noise power. While the first one seems obvious, the latter one is not: the extra noise comes originally from the phase noise of the signal generator. Unlike the carrier interference that can be substantially attenuated by the jammer cancellation loop, the phase noise beyond the bandwidth of either the antenna or the matching network does not get attenuated as effectively. The net result is therefore a severe degradation of the SNR.

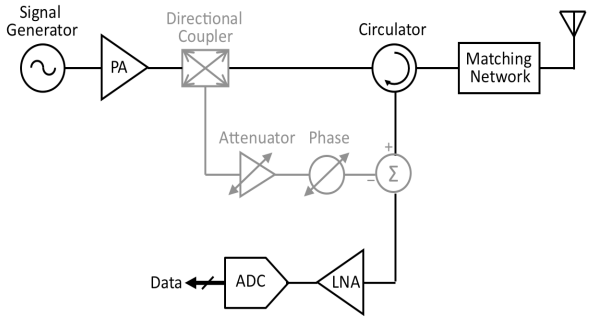

Figure 8. Reader block diagram

V. CONCLUSION

This paper discusses system level perspectives on the design and optimization of miniature neural implants of scalable sizes. Electromagnetic power transfer is identified as the most feasible approach for energy delivery. An alternative communication scheme, Reflective Impulse Radios, is also proposed to address the data transmission challenge. The combined results present the great feasibility of realizing self-contained neural implants down to mm in size.

ACKNOWLEDGMENT

The authors wish to acknowledge the contributions of the students, faculty and sponsors of the Berkeley Wireless Research Center, the support of the Multiscale Systems Center (MuSyC), one of six research centers funded under the Focus Center Research Program, a Semiconductor Research Corporation program, the NSF Infrastructure Grant No. 0403427, and the UC Discovery-Agilent Grant.

REFERENCES

[1] M.A.L Nicolelis, et al., "Chronic, multi-site, multi-electrode recordings in macaque monkeys," Proc. Natl. Acad. Sci. USA 100, pp. 11041–11046, 2003.

[2] Rousche PJ, Normann RA. Chronic recording capability of the Utah Intracortical Electrode Array in cat sensory cortex. J Neurosci Methods 1998;82:1–15.

[3] Polikov VS, Tresco PA, Reichert WM (2005). Response of brain tissue to chronically implanted neural electrodes. J Neurosc Methods 148, pp. 1–18.

[4] Roundy, S.; et al, "Energy Scavenging for Wireless Sensor Networks: with Special Focus on Vibrations." Kluwer Academic Publishers, 2004

[5] N. Mano, "A 280uW cm-2 biofuel cell operating on low glucose concentration," Chem. Commun., issue 19, pp. 2221 – 2223, 2008

[6] Paradiso, J.A.; Starner, T.; , "Energy scavenging for mobile and wireless electronics," *Pervasive Computing, IEEE* , vol.4, no.1, pp. 18- 27, Jan.-March 2*005*

[7] *E K Reilly and P K Wr*ight "Modeling, fabrication and stress compensation of an epitaxial thin film piezoelectric microscale energy scavenging device" 2009 *J. Micromech. Microeng.* 19 095014

[8] R. R. Harrison, et al., "Wireless neural recording with single low-power integrated circuit," *Trans. on Neural Systems and Rehabilitation Engineering***,** pp. 322-329**,** Aug. 2009

[9] A. S. Y. Poon, S. O'Driscoll, and T. H. Meng, "Optimal frequency for wireless power transmission into dispersive Tissue," *Antennas and Propagation, IEEE Transactions on,* vol.58, no.5, pp.1739-1750, May 2010

[10] Mark, Michael; Bjorninen, Toni; Chen, Yuhui David; Venkatraman, Subramaniam; Ukkonen, Leena; Sydanheimo, Lauri; Carmena, Jose M.; Rabaey, Jan M.; , "Wireless channel characterization for mm-size neural implants," *Engineering in Medicine and Biology Society (EMBC), 2010 Annual International Conference of the IEEE* , vol., no., pp.1565-1568, Aug. 31 2010-Sept. 4 2010

[11] M. Mark, T. Björninen, L. Ukkonen, L. Sydänheimo, and J. M. Rabaey, "SAR reduction and link optimizatin for mm-size remotely powered wireless implants using segmented loop antennas," to be presented at the *IEEE Topical Conference on Biomedical Radio and Wireless Technologies, Networks and Sensing Systems,* Phoenix, January 2011

[12] "Questions and answers about biological effects and potential hazards of radiofrequency electromagnetic fields," *OET Bulletin Number 56 (4th Edition August 1999),* FCC

[13] Council Recommendation on the Limitation of Exposure of the General Public to Electromagnetic Fields (0 Hz to 300GHz), *Official Journal of the European Communities,* July 12, 1999.

[14] Sohee Kim; Tathireddy, P.; Normann, R.A.; Solzbacher, F.; , "Thermal Impact of an Active 3-D Microelectrode Array Implanted in the Brain," *Neural Systems and Rehabilitation Engineering, IEEE Transactions on* , vol.15, no.4, pp.493-501, Dec. 2007

[15] R. Muller, S. Gambini, J. Rabaey, "A 0.013mm^2 5µW DC-coupled Neural Signal Acquisition IC with 0.5 V supply", IEEE International Solid-State Circuits Conference, in press, 2011

[16] Mandal, S.; Sarpeshkar, R.; , "Low-Power CMOS Rectifier Design for RFID Applications," *Circuits and Systems I: Regular Papers, IEEE Transactions on* , vol.54, no.6, pp.1177-1188, June 2007

[17] "IEEE standard for safety levels with respect to human exposure to radio frequency electromagnetic fields, 3 kHz to 300 GHz," *IEEE Std C95.1-2005*, 2006

[18] M. Rizk, I. Obeid, S.H. Callendar, P.D. Wolf, "A single-chip signal processing and telemetry engine for an implatable 96-channel neural dta acquisition system," *Journal of Neural Engineering,* vol.4, pp.309-321, 2007

[19] R. Harrison, et al., "A Low-Power Integrated Circuit for a Wireless 100-Electrode Neural Recording System," *IEEE Intl. Solid-State Circuits Conf. (ISSCC) Dig. Tech. Papers*, pp. 554-555, 2006

[20] K. Finkenzeller, *RFID Handbook: Fundamentals and Applications in Contactless Smart Cards and Identification,* John Wiley & Sons, 2003

[21] M. Sasaki, "A 12-mW 500-Mb/s 1.8-µm CMOS Pulsed UWB Transceiver Suitable for Sub-meter Short-range Wireless Communication," *IEEE Radio Frequency Integrated Circuits Symposium,* pp. 593-596, 2008

[22] T. Terada, et al. "A CMOS Ultra-Wideband Impulse Radio Transceiver for 1-Mb/s Data Communications and 2.5-cm Range Finding," *IEEE Journal of Solid-State Circuits (JSSC),* vol. 41, pp. 891-898, 2006

[23] W. Yao, Y. Wang, "Direct antenna modulation − a promise for ultra-wideband (UWB) transmitting," *IEEE MTT-S International Microwave Symposium Digest,* pp. 1273-1276, 2004

[24] S. D. Keller, W. D. Palmer, W. T. Joines, "Direct antenna modulation: analysis, design, and experiment," *IEEE Antennas and Propagation Society International Symposium,* pp. 909-912, 2006

[25] S. D. Keller, *Design and Development of Directly-Modulated Antennas Using High-Speed Switching Devices,* PhD Dissertation, Duke University, 2008